Chapter 5

Quantum heat engine with near-zero irreversible work utilizing quantum skyrmion working substance

5.1 Introduction

Quantum thermodynamics investigates thermodynamic processes at the quantum level [241, 242, 243, 244, 245, 246, 247, 248] and establishes a link between thermodynamics and quantum theory. The practical aspect of quantum thermodynamics is constructing quantum heat engines and studying quantum thermodynamic processes [249, 250, 251, 252, 253, 254, 255, 256, 257, 258, 259]. Quantum heat engines can be incorporated into nano devices and perform work on the nano level. The fundamental aspect of quantum thermodynamics is the study of the role of quantumness in thermodynamic processes, which is highly important for the foundation of quantum statistical mechanics. In the present work, we analyze both fundamental and practical aspects. For a comprehensive understanding of various aspects of quantum thermodynamics and quantum heat engines, the recent literature provides valuable insights [260, 261, 262, 263, 264, 265, 266, 267,

268, 269, 270, 271, 272, 273, 274, 275, 276, 277, 278, 279, 280, 281, 282]. A critical effect of quantumness is the effect of quantum friction. Swift driving of a quantum system leads to quantum multiple inter-level transitions. As a result, a substantial amount of work is wasted in the form of irreversible work. The irreversible work can be reduced by slowing down driving speed of the cycle. However, this reduces the output power of the quantum engine as well. An elegant way to address this issue is to employ adiabatic shortcuts, addition of an extra driving term compensating irreversible losses of quantum origin [283, 284, 285]. Unfortunately, adiabatic shortcuts are hard to construct for experimentally feasible physical systems. In the present study, we address this problem based on the effect of topological protection. We analyzed quantum thermodynamic processes and considered quantum skyrmion as a working body for the quantum Otto cycle. We showed that owing to the topological protection [232, 286], when the system is in the quantum skyrmion phase, the propagated quantum states differ from the initial states only by dynamical and geometrical phases (calculated and presented in Fig. 5.4). Consequently, nondiagonal transition matrix elements are nearly zero leading to near-zero irreversible work. The evolution of the system in the quantum skyrmion phase is adiabatic. Before considering thermodynamic aspects, for the interest of a broad audience, we briefly review the field of quantum skyrmionics. Particle-like topological solitons, particularly skyrmions, exhibit great promise in spintronics applications. Skyrmions were initially discovered in studies of fundamental field theory [116, 117, 118, 121] and subsequently observed in magnetic systems [122, 123, 124, 125, 126, 287, 288].

The underlying physical mechanism responsible for the formation of skyrmion magnetic textures involves the Dzyaloshinskii–Moriya interaction (DMI) or spin frustration, arising from the competition between nearest-neighbor ferromagnetic and next-nearest-neighbor antiferromagnetic exchange interactions. In the field of condensed matter physics, the term “skyrmionics" has emerged as a prominent topic of research [127, 128, 129,

130, 131, 132, 133, 135, 136, 137, 289]. Classical magnetic skyrmions are formed by a collective arrangement of numerous spins. However, recent attention has shifted towards quantum skyrmions [109, 138, 140, 141, 142, 198, 237, 238, 238, 290, 291].

In a recent work [143], a new concept of matter called a “plasmonic skyrmion lattice" was suggested. This lattice is formed within an optical system through the interference patterns of surface plasmon polaritons generated by coherent or incoherent laser sources. The skyrmions, which are topologically nontrivial magnetic structures, become confined to the nodal points of this optical lattice. The underlying mechanism responsible for this confinement is the magnetoelectric (ME) effect [292]. The emergent ferroelectric polarization [237], denoted as $\mathbf{P} = \sum_{\langle i,j \rangle} (\mathbf{e_{ij}} \times \hat{z}).\left(\hat{\mathbf{S}}_i \times \hat{\mathbf{S}}_j\right)$, couples with the electric field of the plasmons, resulting in an effective DMI term characterized by $D = g_{ME}E$. Here, $\vec{e}_{ij}$ represents the unit vector connecting neighboring spins $\hat{\mathbf{S}}_\mathbf{i}$ and $\hat{\mathbf{S}}_\mathbf{j}$, and g_{ME} denotes the constant associated with the magnetoelectric coupling. Experimental observations of skyrmions in a single-phase multiferroic material, Cu_2OSeO_3, have been reported [124]. For insights into the quantum aspects, the work [293] provides relevant information. The noncolinear magnetic spin texture $(\hat{\mathbf{S}}_\mathbf{i} \times \hat{\mathbf{S}}_\mathbf{j})$ is a crucial aspect of the magnetoelectric (ME) effect. Consequently, when an external electric field is applied to a magnetic layer, it selectively couples with skyrmions rather than the majority of the surface layer that exhibits ferromagnetic spin order. This observation opens up new possibilities in the field of quantum thermodynamics. In this study, we propose a novel type of quantum heat engine called the “*plasmonic skyrmion quantum heat engine*." Additionally, previous research [143] has shown that the distances between skyrmions in a plasmonic lattice can be adjusted to the range of 250-300 nm. Consequently, noninteracting skyrmions can be treated as individual modules within the quantum engine. By employing an arbitrary number of skyrmions, the working substance of the plasmonic skyrmion heat engine can be tailored to achieve the desired work and output power. A typical quantum heat cycle

consists of four stages, during which the quantum working body is connected to cold and hot heat baths and externally driven to produce thermodynamic work (Fig. 5.1). In the subsequent sections, we demonstrate that the topological protection of quantum skyrmions nearly eliminates irreversible work. Consequently, the plasmonic quantum skyrmion heat engine does not require adiabatic shortcuts, offering a substantial advantage over other models, which require superconducting circuit networks to achieve adiabatic shortcuts [254]. Skyrmions are stable at temperatures much higher than critical temperature of superconducting circuit networks. As opposite to other topological excitations, skyrmions can be tweezed and confined through the plasmonic modes [219].

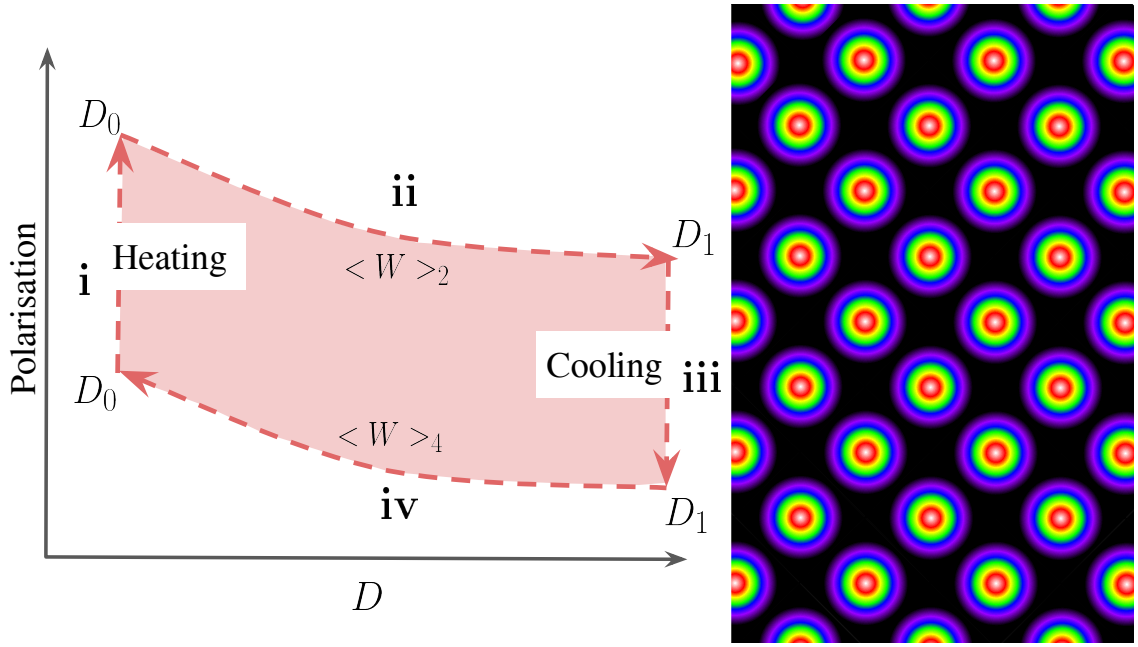

Fig. 5.1 Schematics of the heating/cooling cycle (left) and the plasmonic skyrmion lattice (right).

5.2 Model

Before we explore the thermodynamic properties of a quantum skyrmion we must introduce the theoretical model, as discussed in recent research [237]. Particularly, we consider a

square lattice of interacting quantum spin $1/2$s coupled to classical control fields at its boundary similar to [237]. This model is inspired by the work by Spethmann *et al.* [294], where they modify the film edge of the skyrmion formed by atomic Pd/Fe bilayer on Ir(111) with ferromagnetic Co/Fe patches. This ferromagnetic rim which is the boundary of the skyrmion that we model is referred to as the classical control field. The Hamiltonian of the system is as follows:

$$\hat{H} = \quad -J \sum_{\langle i,j \rangle} (\hat{S}_i^x \hat{S}_j^x + \hat{S}_i^y \hat{S}_j^y) - \Delta \sum_{\langle i,j \rangle} \hat{S}_i^z \hat{S}_j^z \quad -D \sum_{\langle i,j \rangle} (\mathbf{e_{ij}} \times \hat{z}).\left(\hat{\mathbf{S}}_i \times \hat{\mathbf{S}}_j\right). \tag{5.1}$$

With a ferromagnetic coupling constant $J = 1$, the axial Heisenberg anisotropy $\Delta > 0$ and Dzyaloshinskii–Moria interaction (DMI) strength D, where $\vec{e}_{ij}$ is the unit vector pointing from $\vec{\hat{S}}_i$ to $\vec{\hat{S}}_j$. The $\vec{\hat{S}}_i = \frac{\hbar}{2}\hat{\vec{\sigma}}_i$ corresponds to a vector of spin operators (vector of Pauli matrices) $\hat{\vec{\sigma}}_i = \left(\sigma_i^x, \sigma_i^y, \sigma_i^z\right)$. The summation runs over all the unique pairs of nearest neighbors. The last term in the Hamiltonian Eq.C.1: $D \sum_{\langle i,j \rangle} (\mathbf{e_{ij}} \times \hat{z}).\left(\hat{\mathbf{S}}_i \times \hat{\mathbf{S}}_j\right)$ describes coupling between electric field E and ferroelectric polarization $\hat{P} = \sum_{\langle i,j \rangle} (\mathbf{e_{ij}} \times \hat{z}).\left(\hat{\mathbf{S}}_i \times \hat{\mathbf{S}}_j\right)$, where $D = E\gamma_{ME}$ is the effective DM constant and γ_{ME} is the magneto electric coupling. The expectation value $\langle \hat{P} \rangle = Tr(\hat{\rho}\hat{P})$ depends on the eigenvalues and eigenstates of the density operator $\hat{\rho}$. The density matrix changes either by heating or cooling processes or by the driving through the electric field $D = \gamma_{ME}E$. Consequently, the expectation value $\langle \hat{P} \rangle$ changes during the thermal processes (strokes **i** and **iii**) and work production strokes (**ii** and **iv**), see Fig. 5.1. We refer to the works Ref.[257] and Ref.[258] for more details. Importantly, the plasmonic modes in the system only couple with the noncollinear magnetic textures of the skyrmions. By controlling the strength of the DM interaction D through the plasmonic mode E [143], we can tune the parameter $D = g_{ME}E$ and define the region of the skyrmion phase.

5.2.1 Quantum thermodynamic relations

The concepts of thermodynamics are based on the definition of heat and work and the first and second laws of thermodynamics. Interested readers can find details regarding specific facts concerning quantum thermodynamics in the review paper [62]. Here, we refer to the facts that are important for further discussion. For a generic quantum system described by the Hamiltonian $\hat{H}$ and density matrix $\hat{\rho}$, the expectation value of the energy reads $U(\hat{\rho}) = \mathrm{tr}[\hat{\rho}\hat{H}]$. During the thermodynamic stroke $t \in [0, \tau]$, the state of the system, as $\hat{H}(t)$ and $\hat{\rho}(t)$, is changing with time. The change of the energy expectation value is given by the equation:

$$\Delta U = \mathrm{tr}[\hat{\rho}^{(\tau)}\hat{H}^{(\tau)}] - \mathrm{tr}[\hat{\rho}^{(0)}\hat{H}^{(0)}]. \tag{5.2}$$

The average heat absorbed by the system and average work done on the system are given by

$$\begin{aligned} \langle Q \rangle &= \int_0^\tau \mathrm{tr}[\dot{\hat{\rho}}(t)\hat{H}(t)]dt, \\ \langle W \rangle &= \int_0^\tau \mathrm{tr}[\hat{\rho}(t)\dot{\hat{H}}(t)]dt. \end{aligned} \tag{5.3}$$

Thus, the first law of thermodynamics formulated for a quantum system reads:

$$\Delta U = \langle Q \rangle + \langle W \rangle. \tag{5.4}$$

A prototype heat engine contains a working body and, it is alternatively made contact with a cold and hot heat bath for extracting work. Akin to classical heat engines, typically, quantum thermodynamic cycles consist of four strokes: Two strokes are related to the heating or cooling of the working body of the engine, and the other two strokes correspond to the work done by the system or done on the system. The efficiency of any quantum

engine is given by the ratio of the net work [62]: $\langle W_{net} \rangle$ done by the system to the heat supplied to the system Q_{in} from the hot heat bath:

$$\eta = \frac{\langle W_{net} \rangle}{Q_{in}}. \tag{5.5}$$

5.3 Topological protection

For verifying the existence and stability of the quantum skyrmion, we exploit two quantities [295, 296]: the magnitude of the winding parameter Q, and the topological index C defined as follows:

$$\left.\begin{matrix} Q \\ C \end{matrix}\right\} = \frac{1}{2\pi} \sum_{\sigma} \tan^{-1} \left(\frac{\mathbf{n}_i (\mathbf{n}_j \times \mathbf{n}_k)}{1 + \mathbf{n}_i \mathbf{n}_j + (\mathbf{n}_i \mathbf{n}_k)(\mathbf{n}_k \mathbf{n}_j)} \right). \tag{5.6}$$

Here the summation is performed over all elementary triangles formed by nearest-neighbor lattice sites i, j, and k with no overlapping triangles. The stability of the skyrmion is characterized by the winding parameter Q, which is calculated as $\mathbf{n_i} = 2\langle \mathbf{S}_i \rangle / \hbar$, where $\langle \mathbf{S}_i \rangle = (\langle S_i^x \rangle, \langle S_i^y \rangle, where \langle S_i^z \rangle)$ represents the spin expectation value. The topological index C is defined as $\mathbf{n_i} = \langle \mathbf{S}_i \rangle / |\langle \mathbf{S}_i \rangle|$taking the values $C = \pm 1$ for quantum skyrmions.

The DM term for continuous two-dimensional magnetic texture $\mathbf{m}(\mathbf{r})$, $\mathbf{r} = (x, y)$ is akin to the topological action term [297] $S_{top}[\mathbf{m}(\mathbf{r})] = \frac{i\theta}{4\pi} \int dxdy\vec{m}(\partial_x \mathbf{m}(\mathbf{r}) \times \partial_y \mathbf{m}(\mathbf{r}))$ and is invariant under the infinitesimal perturbations $\mathbf{m}(\mathbf{x}) \to \mathbf{m}(\mathbf{x}) + \varepsilon \hat{\mathbf{R}} \mathbf{m}(\mathbf{x})$, ($\hat{\mathbf{R}}$ is the generator of $SO(3)$ group) meaning that $\delta S_{top} = S_{top}[\mathbf{m}(\mathbf{x}) + \varepsilon \hat{\mathbf{R}} \mathbf{m}(\mathbf{x})] - S_{top}[\mathbf{m}(\mathbf{x})] = 0$. The robustness of the action with respect to the infinitesimal perturbations $\delta S_{top} = 0$ means that it cannot be deformed continuously; it is quantized $S_{top}[\mathbf{m}(\mathbf{x})] = i\theta W$, where W is the topological charge. We note that the topological index in Eq.5.6 is a discrete version of the topological charge [238]. In the language of quantum thermodynamics, those small perturbations are akin to quantum friction. Topological entanglement entropy (TEE) is a useful quantity for identifying phases and assessing topological protection, particularly

in larger system sizes [298]. However, in our case, since we are working with a small system size and employing open boundary conditions, TEE does not provide significant insights. As shown in Fig: 5.2(A), we have either a ferromagnetic state with topological index $C = 0$ or a skyrmion state with $C = -1$, depending on the values of the anisotropy parameter Δ, and the electric field D. For $\Delta = 0.25J$, we have a skyrmion $C = -1$ in the whole interval $0 < D < 2J$. In Fig: 5.2(B), we have plotted the winding parameter, Q *vs.* D, which characterizes the robustness or the stability of a quantum skyrmion state [237] to withstand transition to trivial phase.

In the following analysis, we will focus on the skyrmion state and investigate the first thermodynamic quantity of interest, namely non-equilibrium work. In what follows, we show that irreversible work in the quantum skyrmion phase is too small. This effect is related to the marginal values of transition matrix elements, the structure of the system's eigenstates in the quantum skyrmion phase, and eventually topological protection (topological protection leads to the formation of skyrmion structures and the specific type of eigenstates).

5.4 The quantum Otto cycle

To describe the state of the system, we define the thermal density matrix as $\hat{\rho}_0 = Z^{-1}\sum_n e^{-\beta\mathscr{E}_n(0)}\,|\varphi\rangle_n\,\langle\varphi|_n$, where β is the inverse temperature, $Z = \sum_n e^{-\beta\mathscr{E}_n(0)}$ is the partition function, $|\varphi\rangle_n$ represents the eigenfunctions of the system described by Eq.(C.1), including low-lying skyrmionic states [238], and E_n are the corresponding eigenvalues. We drive the system by manipulating the plasmonic field $D(t)$ in time, specifically within the skyrmion region. The skyrmion, acting as the working substance, produces thermodynamic work, which can be quantified as $\langle W\rangle = \langle W_{\rm ir}\rangle + \Delta F$ where $\langle W\rangle$ represents the total work produced by the skyrmion quantum heat engine, $\Delta F = -\frac{1}{\beta}\ln(Z_f/Z_0)$ corresponds to the change in free energy during the stroke, and $\langle W_{\rm ir}\rangle$ denotes the irreversible work. $\langle W_{\rm ir}\rangle$ arises due to quantum inter-level

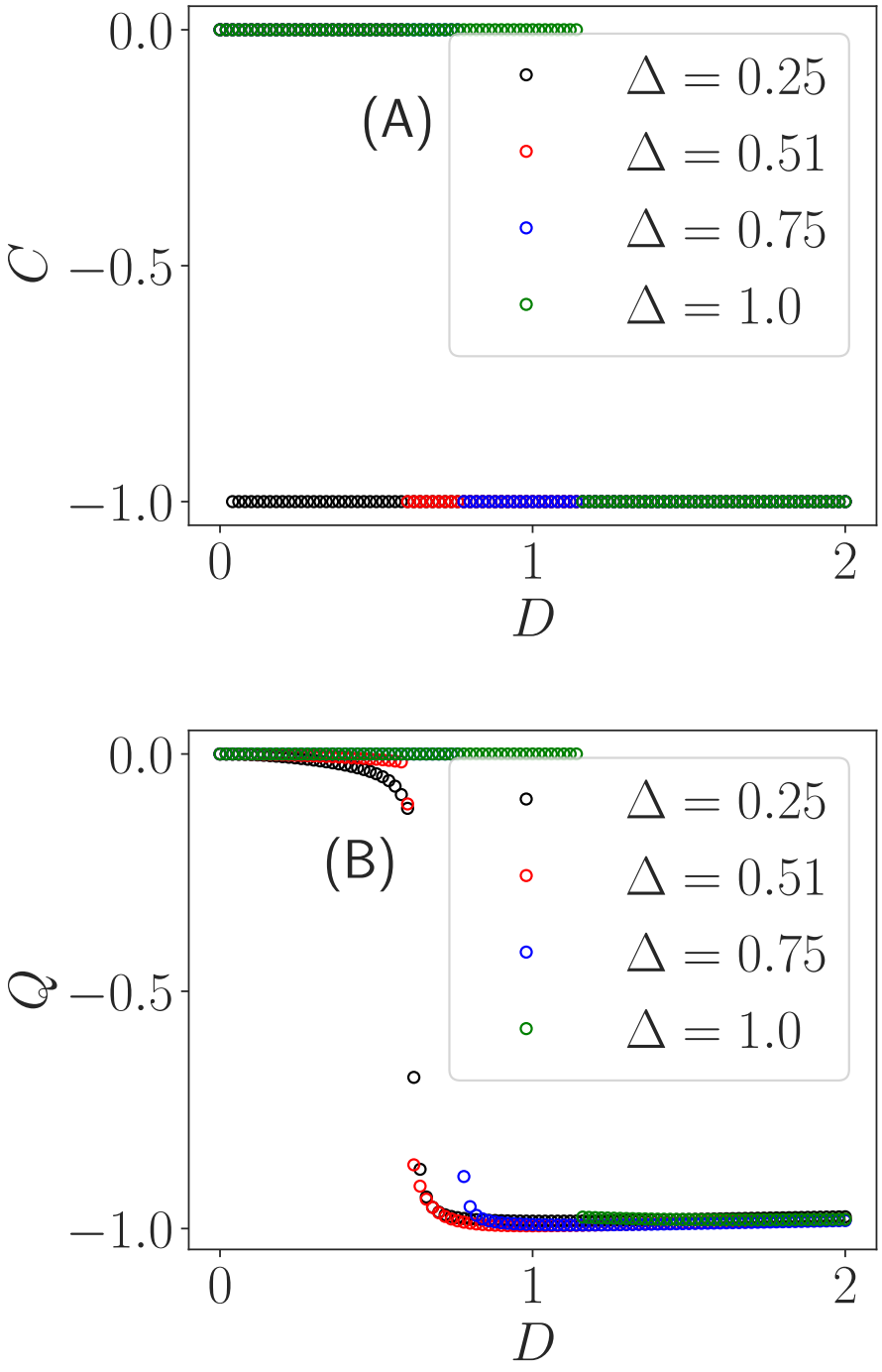

Fig. 5.2 (A) Topological Index, *C vs. D* magnitude for various anisotropy constant values. (B) Winding parameter, *Q vs. D* magnitude for various anisotropy constant values.

transitions occurring in finite-time processes. It represents the dissipated or wasted work and can be quantified by the deficit between the produced work and the change in the free energy of the system [251, 255, 258, 263, 264]. The quantum Otto cycle consists of the following four strokes, as illustrated in Fig. 5.1:

i) Thermalization at high temperature: At the beginning of the cycle, the magnetic texture (skyrmion) is in contact with a high-temperature bath at temperature T_H. By applying an electric field E_0, the magnetoelectric coupling results in a change in the Dzyaloshinskii-Moriya interaction parameter, $D_0 = g_{ME}E_0$, at time $t = 0$. During this stroke, the skyrmion absorbs heat Q_{in} from the high-temperature bath. In [299] the flow of heat is shown to be affected by the DMI interaction strength.

ii) Mean work extraction: The electric field is changed from E_0 to E_1 during this stroke, where $E_1 > E_0$. This change in the electric field corresponds to a change in the Dzyaloshinskii-Moriya interaction parameter, $D_1 = g_{ME}E_1$, at time $t = \tau$. The duration of this stroke is denoted by τ. The mean work performed by the system reads [300] $\langle W\rangle_2 = \sum_{m,n}(\mathscr{E}_m(\tau) - \mathscr{E}_n(0))p^{\tau}_{m,n}p^0_n$, where $p^{\tau}_{m,n} = |\langle\mathscr{E}_n(\tau)|\hat{U}(\tau)|\mathscr{E}_m(0)\rangle|^2$ is the inter-level transition probability, $\hat{U}(\tau) = e^{-i/\hbar\int_0^{\tau}H(t)dt}$ is the time evolution operator, $p^0_n = e^{-\beta_H\mathscr{E}_n(0)}Z(\beta,\mathscr{E}(0))$, $p^{\tau}_n = \sum_m p^{\tau}_{m,n}p^0_m$ are level populations of the propagated state. $\mathscr{E}_n$ represents the energy eigenvalues, $\beta_H = 1/T_H$ is the inverse temperature of the hot bath, and $Z(\beta_H,\mathscr{E}(0)) = \sum_n e^{-\beta_H\mathscr{E}_n(0)}$ is the partition function at the initial energy. We note that a finite-time driving process concerning the complex quantum systems is a highly non-trivial problem [301].

iii) Cooling through a cold bath: In this stroke, the system is brought into contact with a cold bath at temperature T_L. The cooling process takes place, allowing the system to release heat to the cold bath.

iv) Return to the initial state: The electric field(DMI) is steered back from $E_1, (D_1)$ to the initial values $E_0, (D_0)$ during this stroke. We calculate The mean work again through [300] $\langle W\rangle_4 = \sum_{m,n}(\mathscr{E}_m(\tau) - \mathscr{E}_n(0))p^{\tau}_{m,n}p^0_n$. However, now $\beta_L = 1/T_L$ is the inverse

temperature of the cold bath, and $Z(\beta_L, \mathscr{E}(\tau)) = \sum_n e^{-\beta_L \mathscr{E}_n(\tau)}$ is the partition function at the final energy. We note that during the stroke $[0,t]$, the dynamic of the system is unitary. Therefore, there will be no immediate losses during the unitary driving stroke. The losses may occur when the non-equilibrium density matrix $\hat{\rho}_t$ relaxes after the end of the stroke. This question is described in detail in the recent work [302]. Strokes **i** and **iii** are thermalisation strokes and no work is done on or by the system.

For non-ideal processes, the deficit between $\langle W \rangle$ and the change of the free energy can be accounted for the $\langle W_{\rm ir} \rangle$ [283] $\langle W \rangle = \langle W_{ir} \rangle + \Delta F$. Practically, $\langle W_{\rm ir} \rangle$ can be calculated using the quantum relative entropy for two density matrices $\hat{\rho}_t$ and $\hat{\rho}_t^{eq}$ which is given by [300, 303]:

$$\begin{aligned} \langle W_{ir} \rangle &= \frac{1}{\beta} S\left(\hat{\rho}_t \| \hat{\rho}_t^{eq}\right), \\ S\left(\hat{\rho}_t \| \hat{\rho}_t^{eq}\right) &= \sum_n p_n^0 \ln p_n^0 - \sum_{n,m} p_n^0 p_{m,n}^{\tau} \ln p_n^{\tau}. \end{aligned} \tag{5.7}$$

Here $\hat{\rho}_t =$ and $\hat{\rho}_t^{eq} = e^{-\beta \hat{H}(t)} / Tr\left[e^{-\beta \hat{H}(t)}\right]$ are non-equilibrium and equilibrium density matrices. From Eq.(5.7) it is easy to see that $\langle W_{\rm ir} \rangle$ is zero if $p_{m,n}^{\tau} = \delta_{nm}$ (see Fig. 5.3 and the description).

The irreversible work $\langle W_{ir} \rangle$ is influenced by the driving protocol and tends to increase for faster driving rates. In our setup, we keep the starting and ending points of the plasmonic electric field fixed at D_0 and D_1, respectively, and we achieve the variation of D by implementing a linear quench in the Hamiltonian with different rates v. The functional dependence of D on time during the quench is assumed to be as follows: $D_t = D_0 + (D_1 - D_0)vt$.

Our main statement is that owing to the topological protection irreversible work becomes nearly zero at the end of the stroke, this can be verified numerically for an appropriate choice of driving rate. Let us look at the quantities entering the expression of

irreversible work:

$$\langle W_{ir}\rangle = \frac{1}{\beta} S\left(\hat{\rho}_t || \hat{\rho}_t^{eq}\right), \tag{5.8}$$

$$S\left(\hat{\rho}_t || \hat{\rho}_t^{eq}\right) = \sum_n p_n^0 \ln p_n^0 - \sum_{n,m} p_n^0 p_{m,n}^t \ln p_n^t, \tag{5.9}$$

$$\hat{\rho}_t^{eq} = e^{-\beta \hat{H}(t)} / \mathrm{Tr}\left[e^{-\beta \hat{H}(t)}\right], \tag{5.10}$$

$$\hat{\rho}_t = \hat{U}^{-1}(t)\hat{\rho}(0)\hat{U}(t),\ \hat{U}(t) = e^{-i/\hbar \int_0^t \hat{H}(\tau) d\tau}, \tag{5.11}$$

$$p_{m,n}^t = |\langle \mathscr{E}_n(\tau)| \hat{U}(t) |\mathscr{E}_m(0)\rangle|^2, \tag{5.12}$$

$$Z(\beta, \mathscr{E}(0)) = \sum_n e^{-\beta \mathscr{E}_n(0)}, \tag{5.13}$$

where

$$p_n^0 = e^{-\beta \mathscr{E}_n(0)} Z(\beta, \mathscr{E}(0)),\ p_n^t = \sum_m p_{m,n}^t p_m^0. \tag{5.14}$$

We steer the DMI constant from D_0 at $t = 0$ to D_1 at t and calculate $p_{m,n}^t$. The irreversible work is small or zero if $p_{m,n}^t \approx \delta_{nm}$. The results of numerical calculations are shown in Fig. 5.3. The obtained result means that the propagated state $|\psi(t)\rangle = \hat{U}(t)|\mathscr{E}_n(0)\rangle$ is different from the quantum skyrmion state $|\mathscr{E}_n(\tau)\rangle$ only by geometric and dynamical phases, meaning that:

$$|\psi(t)\rangle = \hat{U}(t)|\mathscr{E}_n(0)\rangle = \exp\left[-\frac{i}{\hbar}\int_0^t d\tau \mathscr{E}_n(\tau) - \int_0^t d\tau \langle \mathscr{E}_n(\tau)|\partial_\tau \mathscr{E}_n(\tau)\rangle\right] |\mathscr{E}_n(\tau)\rangle, \tag{5.15}$$

Here, $\left[-\frac{i}{\hbar}\int_0^t d\tau \mathscr{E}_n(\tau) - \int_0^t d\tau \langle \mathscr{E}_n(\tau)|\partial_\tau \mathscr{E}_n(\tau)\rangle\right]$ is the total phase introduced to the equilibrium state under the evolution, and

$$\phi_{dyn} = -\frac{i}{\hbar}\int_0^t d\tau \mathscr{E}_n(\tau)$$

and

$$\phi_{geo} = \int_0^t d\tau \langle \mathscr{E}_n(\tau)|\partial_\tau \mathscr{E}_n(\tau)\rangle$$

are called the dynamical and geometrical phases, respectively.

We checked the validity of Eq.(5.15) by numerical calculations and observed that the propagated states differ only by the geometrical and the dynamical phases from the initial state. Results are plotted in Fig.5.4. The zero transition matrix elements, $p^t_{m,n} \approx \delta_{nm}$ lead to constant occupation probabilities during the strokes **ii** and **iv** (see appendix D.1), and accordingly the entropy remains invariant during these strokes [304, 305]. Heat flow and its direction in a quantum system are affected by the temperature gradient experienced [299, 306]. Taking into account that irreversible work $\langle W_{ir}\rangle$ in our case is very small, when calculating the efficiency (Work output / Heat input) of the skyrmion quantum Otto cycle, we exploit the formula:

$$\eta = \frac{\Delta F_2 + \Delta F_4}{Q_{in}}. \tag{5.16}$$

Here $\Delta F_2 = -\frac{1}{\beta_H}\ln\left(Z(T_H,D_1)/Z(T_H,D_0)\right)$ and $\Delta F_4 = -\frac{1}{\beta_L}\ln\left(Z(T_L,D_0)/Z(T_L,D_1)\right)$. T_L, T_H are temperatures of the cold and hot baths respectively. $Q_{in} = \sum_n \mathscr{E}_n(D_0)\left(P_n(T_H,D_0) - P_n(T_L,D_0)\right)$ is the heat pumped into the working substance and $P_n(T_H,D_0) = Z^{-1}(T_H,D_0)e^{-\mathscr{E}_n(D_0)/T_H}$, $P_n(T_L,D_0) = Z^{-1}(T_L,D_0)e^{-\mathscr{E}_n(D_0)/T_L}$ are level populations.

Because the working body in our study is the topological soliton, i.e., a quantum skyrmion with nontrivial spectral properties, this leads to certain complications when calculating efficiency. If our spectrum were akin to the spectrum of a linear oscillator $E_n^\tau - E_m^\tau = (E_n^0 - E_m^0)/\alpha$, taking into account the definitions of heats Q_{in} and Q_{out} we could deduce an expression for efficiency identical to the classical result from the work [250], $\eta = 1 - \omega_c/\omega_h$, with $\omega_c = E_n^\tau - E_m^\tau$, $\omega_h = E_n^0 - E_m^0$. From Fig. 5.5, we see that the efficiency of the quasi-static cycle reaches 45% for the specified set of parameters and is quite high. The choice of parameters was based on two key factors. First is the stability of the skyrmion, given by Q, and the second is the entropy production, governed by parameters leading to zero $\langle W_{ir} \rangle$. We may also consider a case where thermodynamic processes involving work extraction *i. e.* process **ii** and process **iv** are performed in finite time. In such a case, the system could not reach equilibrium with the baths, leading to near-zero irreversible work [305]. In Fig. 5.5 , we have shown the efficiency for this case considering the effect of the near-zero irreversible work, as follows:

$$\eta_{ir} = \frac{\Delta F_2 + \Delta F_4 - (W_2^{ir} + W_4^{ir})}{Q_{in}} \tag{5.17}$$

As we see, η_{ir} is slightly smaller than quasi-static efficiency η, owing to the role of near-zero non-diagonal transition matrix elements ($p_{mn}^\tau \sim 0$) that leads to a small energy loss. In conclusion, the model we explored shows excellent potential to be considered for a heat engine. The application of quantum thermodynamics to helical spin systems was studied earlier in the work [257]. A thin magnetic film with skyrmions can be deposited on a non-magnetic slab and thermalized through thermal phonons. The spin-phonon thermalization process in the helical spin texture is described in detail in the earlier work [258]. Analysis based on the Lindbladian approach showed that the relaxation is very fast with relaxation time of the order of $\tau_{th} \approx 0.02$ [ps], for $\hbar/J = 0.1$ [ps], where J is the exchange constant. We consider dimensionless time measured in the units of $\hbar/J$,

$D_0 = 0$, $D_1 = 2J = 2$, $v_2 = 2$. Therefore, the stroke duration $\Delta t_2 = \frac{1}{v_2}\frac{\hbar}{J} = \frac{\hbar}{2J}$. The output power is given by $\mathscr{P} = W_{tot}/\tau_{cycle} = NJ/\hbar$, where N is the number of the skyrmions in the plasmonic lattice separated from each other by a distance larger than skyrmion's radius.

5.5 Finite time thermodynamics and thermalization

The application of quantum thermodynamics to helical spin systems was studied earlier in the work Ref. [257]. Magnetic thin film with skyrmions can be deposited on non-magnetic slab and thermilized through the thermal phonons Fig. 1, in Ref. [257]. The spin-phonon thermalization process in the helical spin texture is described in detail in the earlier work Ref.[258]. Analysis based on the Lindbladian approach showed a fast relaxation time of the order of $\tau_{th} \approx 0.02$ [ps], for $\hbar/J = 0.1$ [ps], where J is the exchange constant. For plasmonic skyrmion heat engine we follow the driving protocol $D(t) = D_0 + (D_1 - D_0)vt$, where v characterizes the swiftness of the driving protocol $H[D(t)]$. When the distance between skyrmions in the plasmonic skyrmion lattice, r is larger than the radius of the skyrmion, ρ or $\rho/r < 1$ (typically $\rho = 30$ nm while $r = 250 - 300$ nm and larger) skyrmions do not interact; in essence, they are the independent "cylinders" of the heat engine. The total produced work scales with the number of the skyrmions $W_{tot} = \langle W \rangle N$, where $\langle W \rangle$ is the work done by a single skyrmion. We considered different driving rates, and even in the case of fast driving, the ratio between total and wasted work is marginal $\langle W_{ir} \rangle / \langle W \rangle \ll 1$. Thus, the properties of the plasmonic lattices allow us to construct a cycle with many cylinders (skyrmions), increasing the production of work in this way.

The output power is given by $\mathscr{P} = W_{tot}/\tau_{cycle}$. The main part of the cycle duration τ_{cycle} comes from the work strokes **ii** and **iv** and is in the order of $2\Delta t_1 = \frac{2}{v_1}\frac{\hbar}{J} = \frac{2\hbar}{J}$. Owing to the absence of irreversible work, we can minimize the duration of the work strokes and enhance the power, and topological protection of the skyrmions allows us to construct a

fast cycle and enhance the power of the engine. The output power from the cycle according to the Eq. 5.7 and $\langle W_{\mathrm{ir}}\rangle/\langle W\rangle \ll 1$, and calculated $\langle W\rangle = \Delta F = 2$ is,

$$\mathscr{P} = \frac{NJ\Delta F}{2\hbar} = \frac{NJ}{\hbar} \tag{5.18}$$

Here ΔF is the change of the free energy of a single skyrmion over the stroke and it is numerically estimated, and N is the number of skyrmions. Power of quantum heat engines has shown to be affected significantly by the number of qubits involved [307]; by controlling the number of plasmonic skyrmions the system shows potential to achieve desired output powers.

5.6 Summary

Quantum heat engines are one of the intriguing problems handled in quantum thermodynamics. The output from a nano-scale quantum heat engine is affected by quantum friction caused by the inter-level transitions. Conventionally, this problem is dealt with by introducing shortcuts to adiabaticity. Quantum skyrmion working substance can overcome quantum friction thanks to the innate properties of its eigenstates. The near-zero irreversible work done implies a practically zero quantum friction loss. The heat engine model we proposed shows efficiencies over 45%. In the present work, we proposed to utilize plasmonic modes to control distances between magnetic skyrmions. Here, topologically protected objects are magnetic skyrmions confined through the plasmonic modes [143]. Our model can be realized in materials with magnetoelectric coupling, e.g., Cu_2OSeO_3 [124]. We note that in the materials with magnetoelectric coupling, the Dzyaloshinskii-Moriya interaction (DMI) is the essence of the product between the external electric field E and magnetoelectric constant $D = Eg_{ME}$. Magnetoelectric coupling allows us to construct a unique method: The working substance of the quantum heat engine is formed by the confined magnetic

skyrmions and driven by an external electric field. DMI is essential for the formation of magnetic topological excitations. However, in most cases, magnetic vortices and other topological excitations appear owing to the intrinsic DMI constant, when DMI is a characteristic constant of the particular material and cannot be controlled by an external electric field. Skyrmions in the materials with magneto-electric coupling can be captured and fixed like cold atoms in the optical lattices [219], the other topological excitations can not. This makes our proposal experimentally feasible for realistic materials Cu_2OSeO_3 [124]), moreover, makes the working body unique. Neither of the other topological solitons except the skyrmions considered in our study can suit this purpose. Overall, in the end, we summarize the main features of our quantum heat engine as follows:

- Topologically protected quantum heat engine is practically free of irreversible work and does not need a shortcut of adiabaticity.
- Our model is an experimentally feasible platform and can be realized in magnetic materials with magneto-electric coupling.
- Regarding the design aspect: Our engine can be constructed with the desired number of skyrmions.
- Regarding control and functionality: The engine is controlled by an external electric field, which is a certain advantage.
- Regarding robustness of the system and stability at finite temperatures: The electron-phonon interactions (spin-phonon interactions) are not a problem for skyrmions. Skyrmions are stable at reasonably high temperatures about $T = 100$K [219].

We note that skyrmions are stable and topologically protected solitons. However,the skyrmion phase exists in a certain combination of parameters (exchange constant J, magnetic field B, and DMI D). Steering the DMI constant or magnetic field values may lead

to a transition into the non-skyrmion phase, i.e., into a ferromagnetic ground state. For example, we refer to the dynamical phase transition into the non-skyrmion phase studied in [298]. The same argument also applies to the plasmonic skyrmion lattice phase, which exists for the same combination of parameters as individual skyrmion.

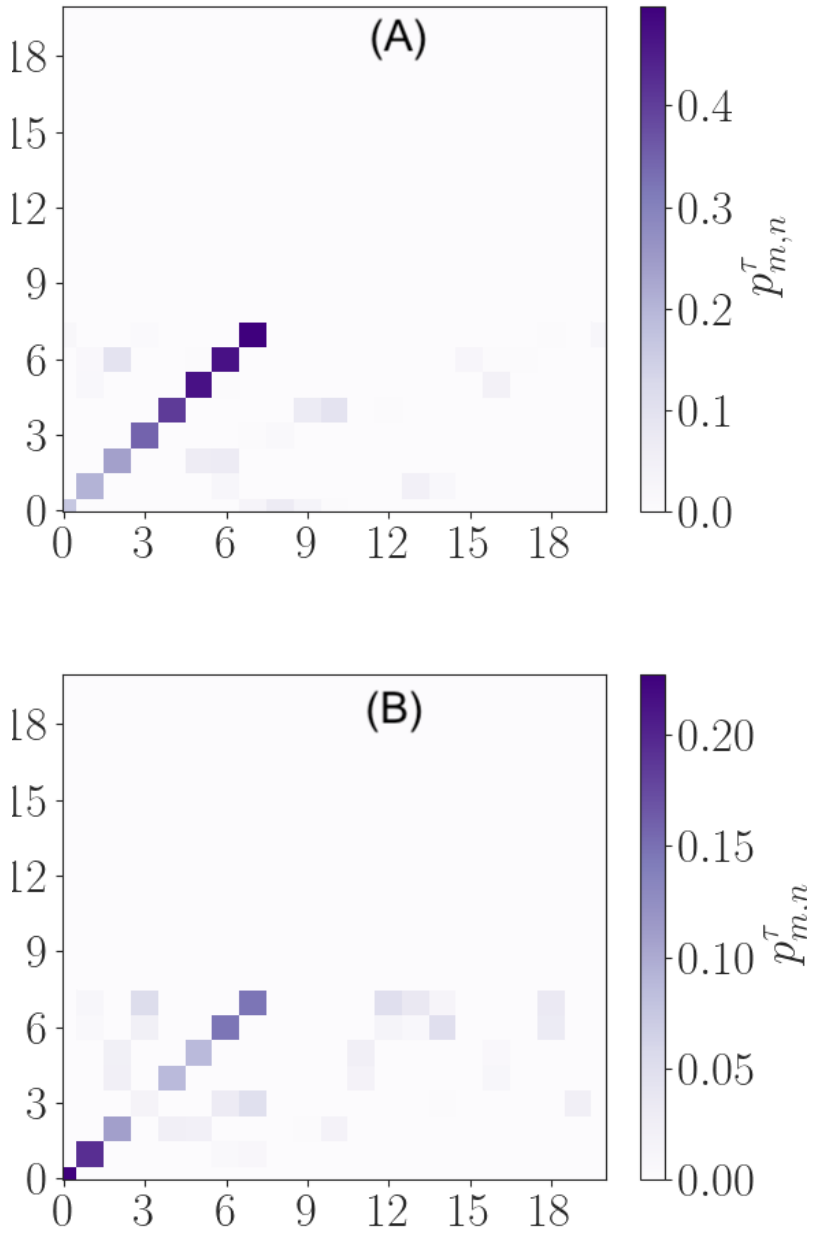

Fig. 5.3 (A) An instance of $p^{\tau}_{m,n}$ is plotted for the first few eigenstates for $\Delta = 0.25J$, $D_0 = 0.0J$ and $D_1 = 0.4J$. We see that only $m = n$ terms have a significant contribution. Here, the initial state is a skyrmion state, and it is evolved within the parameter range where the system remains in the skyrmionic ground state. (B) Here we plot the same quantity for $\Delta = 0.75J$. At $\Delta = 0.75J$ the irreversible entropy tends to settle at a large value after a similar evolution process as in (A). Here we see that the diagonal terms have diminishing magnitude, also off-diagonal terms have significant contribution compared to (A).

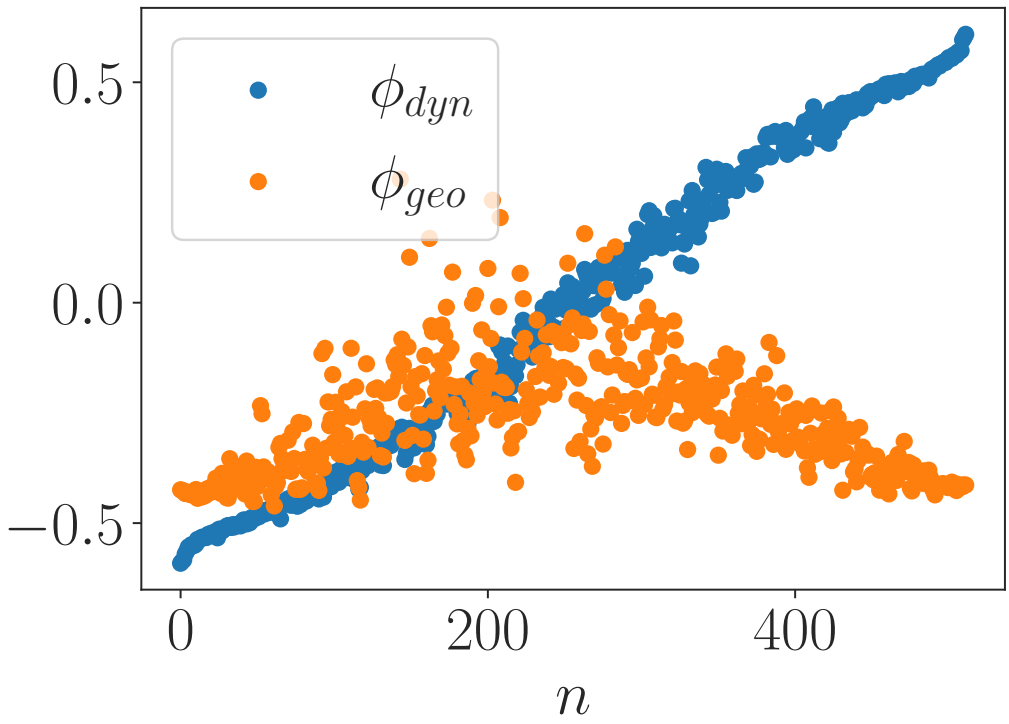

Fig. 5.4 Geometrical and dynamical phases obtained by wave functions during the adiabatic evolution in the skyrmion phase. Results are obtained for different n^{th} states.

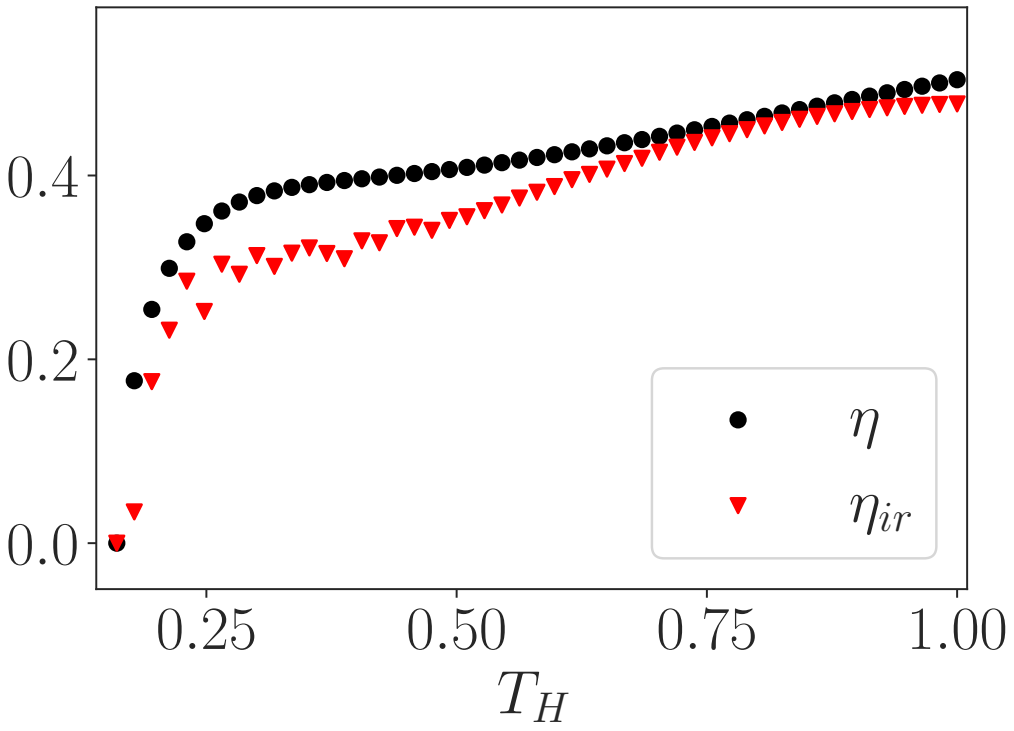

Fig. 5.5 The efficiency of the quasi-static plasmonic skyrmion quantum heat engine η, and efficiency of the finite time cycle which includes effect of the small irreversible work η_{ir} as a function of temperature of the the hot bath $T_H > T_L$. $D_0 = 0J$, $D_1 = 2J$, $T_L = 0.14$, $\Delta = 0.25J$.